https://doi.org/10.3311/PPch.40897

Periodica Polytechnica Chemical Engineering, 69(3), pp. 403–416, 2025

Integration of Simulation and Experimental Approaches for Optimizing TiO_2 Nanowire/Fe_2O_3 Modified Polyethersulfone Membranes in Dye Removal Applications

Mouna Mansor Hussein[1], Qusay F. Alsalhy[2*], Mohamed Gar Alalm[3], Mohamed M. El-Halwany[4,5]

[1] Environmental Engineering Management and Technology, Chemical and Environmental Engineering Department, Faculty of Engineering, Mansoura University, Elgomhouria St., El-Mansoura 35516, Egypt
[2] Membrane Technology Research Unit, Chemical Engineering Department, University of Technology-Iraq, Alsinaa Street 52, 10066 Baghdad, Iraq
[3] Public Works Engineering Department, Faculty of Engineering, Mansoura University, Elgomhouria St., El-Mansoura 35516, Egypt
[4] Department of Mathematics and Physics Engineering, Faculty of Engineering, Mansoura University, Elgomhouria St., El-Mansoura 35516, Egypt
[5] Chemical Engineering Department, Faculty of Engineering, Mansoura National University, Elgomhouria St., El-Mansoura 35516, Egypt
[*] Corresponding authors, e-mail: qusay.f.abdulhameed@uotechnology.edu.iq

Received: 05 May 2025, Accepted: 21 August 2025, Published online: 01 September 2025

Abstract

This study aimed to mimic and optimize polyethersulfone (PES) membrane performance for dye separation applications. Bulk modification was conducted, harnessing titanium dioxide nanowire/iron oxide (TiO_2 NW/Fe_2O_3) to improve water flux, dye removal efficiency, and antifouling properties. Membranes were fabricated with varying nanostructure concentrations (0.1-0.7 g) and examined under different pH levels (3-12) and dye concentrations (25-100 mg/L). Utilizing the response surface methodology (RSM), the process conditions optimized with ANOVA confirmed the adopted model reliability (R^2 = 0.9668 for flux, 0.9809 for rejection). Experimental results revealed that 0.7 g of TiO_2 NW/Fe_2O_3 achieved the highest performance, recording 93 L/m^2·h flux and >99% naphthol blue black dye rejection. Besides, increasing nanostructure content has enhanced the membrane porosity and hydrophilicity. Meanwhile, acidic conditions (pH 3-5) facilitated stronger dye–membrane interactions, while alkaline pH reduced the retention efficiency. Simulation results validated the experimental findings, bestowing deeper insights into the dye separation mechanisms. These findings highlighted the potential of TiO_2 NW/Fe_2O_3-modified PES membranes as a promising candidate for wastewater treatment applications.

Keywords

membrane optimization, Fe_2O_3 nanoparticles, TiO_2 nanowires, dye separation, nanocomposite membranes, response surface methodology

1 Introduction

Wastewater dye contamination has become recognized as an urgent ecological issue, particularly due to its prevalence in effluents from industries like textiles, food production, paper manufacturing, and printing. These industrial processes release dye-laden wastewater, which, if not properly treated, can lead to numerous adverse effects on aquatic ecosystems and water usability. Elevated dye concentrations in water not only impair its suitability for industrial and domestic purposes but also decrease light penetration, thereby inhibiting aquatic plant growth and natural self-purification processes. Furthermore, dyes in wastewater pose serious risks to aquatic life, particularly fish [1]. The textile industry is especially notorious for its water consumption, using substantially more water than many other industrial sectors [2]. The wastewater generated is rich in pollutants, necessitating proper treatment prior to discharge. With over 100000 commercially readily available dyes and an annual production exceeding 700000 tonnes, dye wastewater poses a unique challenge due to the chemical resilience of these compounds. Their complex synthetic structures make them resistant to fading from light exposure, water, and various chemicals, complicating their breakdown in the environment. Dyes are classified into several categories – acidic, basic, disperse, azo, anthraquinone, diazo, and metal-complex – each presenting its own challenges for decolorization and decomposition. Without adequate treatment, these dyes

Cite this article as: Hussein, M. M., Alsalhy, Q. F., Gar Alalm, M., El-Halwany, M. M. "Integration of Simulation and Experimental Approaches for Optimizing TiO_2 Nanowire-Fe_2O_3 Modified PES Membranes in Dye Removal Applications", Periodica Polytechnica Chemical Engineering, 69(3), pp. 403–416, 2025. https://doi.org/10.3311/PPch.40897

can significantly harm the environment [3, 4]. Consequently, meeting stringent environmental regulations has driven researchers to seek effective and economical methods for treating dye-contaminated wastewater.

Significant research has been dedicated to developing innovative techniques for dye removal, ranging from adsorption and oxidation processes to photocatalysis, biological treatments, and membrane separation technologies [5]. However, conventional separation techniques such as ozonation, hydrogen peroxide/UV, bleaching, and electrochemical have proven inadequate as a result of the complex aromatic structures of many textile dyes, which are highly resistant to degradation. These compounds are particularly stable against light exposure, oxidizing agents, and aerobic digestion. As a result, there has been increasing interest in pressure-driven separation membrane processes. They enable the potential of water reuse and the recovery of important waste substances, besides too high dye removal efficiency, such as dyes. Recent advances in both technology and cost-efficiency have further solidified membrane systems as a viable option for industrial wastewater treatment [1].

Membrane processes have gained widespread use in textile wastewater treatment due to their advantages over conventional methods [2]. Nonetheless, all membrane processes have to deal with a scenario of deteriorating permeate flux induced by foulant buildup on the membrane surface [6]. This phenomenon, known as concentration polarization, exacerbates membrane fouling. To address this, various strategies have been proposed, including membrane surface modification, physical cleaning techniques, optimization of operating conditions, the use of antifouling agents, hybrid membrane processes, feed water pretreatment, advanced cleaning techniques, and dynamic membranes. These approaches focus on modifying the bulk or surface properties of membranes to improve their performance.

With the advent of nanotechnology, surface modification using nanomaterials has garnered significant attention for enhancing membrane characteristics and imparting desirable hydrophilic properties [7, 8]. Membranes containing nanomaterials such as carbon nanotubes, zinc oxide, graphene oxide, copper, silver, and titanium dioxide have demonstrated the potential to overcome limitations associated with traditional membrane processes [8–10]. The incorporation of nanofillers into polymeric membranes has been shown to enhance hydrophilicity, improve dye rejection efficiency, increase fouling resistance, and boost thermal and mechanical stability [11–14]. Notably, combining multiple nanomaterials into a single nanocomposite structure has yielded further improvements in membrane performance. Studies indicate that these composite materials not only retain the properties of individual nanomaterials but also exhibit novel functionalities. For example, TiO_2/Fe_2O_3 nanocomposites have demonstrated superior photocatalytic activity for decolorizing dyes such as titan yellow (TY) and methyl orange (MO) under UV light [15]. Similarly, biosynthesized ZnO/CuO nanocomposites have shown effective removal of congo red (CR) dye, achieving a removal capacity of 90.14 mg/g [16]. These findings suggest that nanocomposite materials offer cost-effective and environmentally sustainable solutions for industrial wastewater treatment, particularly in water purification and pollution control applications.

Despite the advanced state of nanocomposite membrane fabrication, the need for optimizing the operation variables is crucial for an efficient and sustainable application. Optimized operational parameters can diminish membrane fouling and enhance membrane characteristics and life span indeed [17–20]. Considering the many variables and interactions influencing membrane performance, the design of experiment (DOE) approach can endow a significant solution to achieve these desired results. Such a powerful example harnessed to optimize process parameters is response surface methodology (RSM) [18, 21]. RMS is an excellent resource for minimizing the number of tests and optimizing process parameters to bestow minimal time and material expenses. It generates results that are particularly reliable and effective and are statistically anticipated [21]. As a mathematical and statistical approach, RMS can deal with multiple factors and endow significant improvement to any membrane process application through developing and optimizing the experimental process if compared to the "one-factor at a time" method [22]. As a result, RSM determines relationships among variables and the impact they have on one or more measured responses alongside offering the optimal level for each variable [23].

This work presents an extension to our previous work, which explored the potential of using hybrid TiO_2 nanowires and Fe_2O_3 nanoparticles as a single nanocomposite to modify polyethersulfone (PES) membranes and improve dye separation performance for naphthol blue black (NBB) dye. The current study integrated RSM approaches to optimize the modified membranes' performance. This was conducted by applying RSM to assess the impact of TiO_2 NW/Fe_2O_3 loading, pH, and dye concentration on the final performance of nanocomposite membranes, aiming to optimize operational conditions for maximum dye rejection and water flux. By incorporating a range of hybrid nanostructures into the polymeric matrix, we aim to optimize the amount of composite material used in the membrane modification process. The integration of RSM into membrane development for wastewater treatment not only accelerates experimental workflows but also leads to statistically validated models that guide the fabrication of high-performance membranes tailored for specific dye contaminants.

2 Experimental

2.1 Preparation of nanostructure and hybrid nanocomposite membranes

Detailed information on the adopted synthesis process of the composite nanostructure can be found elsewhere [24]. Besides, a full characterization confirming the successful fabrication of the TiO_2 NW/Fe_2O_3, including pore size, FTIR, SEM and EDX and XRD analysis, are provided in our recently published work [25].

Meanwhile, the traditional phase inversion approach has been adopted to fabricate neat and TiO_2 NW/Fe_2O_3–PES nanocomposite membranes. Briefly, 2 wt.% of polyethylene glycol (PEG) and a certain amount of TiO_2 NW/Fe_2O_3 were dispersed in dimethylformamide (DMF) solvent via sonication for 1 h. Later, 20 wt.% of PES was added to the solution and stirred continuously for 5 h at 50 °C. The obtained casting solution was then degassed under vacuum conditions to eliminate air bubbles. The dope casting solution was then cast onto a clean glass substrate with a 200 µm clearance gap using an automatic thin film applicator. The membranes were directly placed in a water bath for coagulation. Finally, the membranes were rinsed with deionized (DI) water and stored for future use.

Table 1 lists the specific membrane compositions harnessed in the current work.

Table 1 Casting solutions for the neat PES and TiO_2 NW/Fe_2O_3 modified membranes

Membrane codes	PES (wt%)	PEG (wt%)	DMF (wt%)	TiO_2 NW/Fe_2O_3 (g)
M0	20	2	78	0
M1	20	2	77.99	0.01
M2	20	2	77.97	0.03
M3	20	2	77.95	0.05
M4	20	2	77.93	0.07
M5	20	2	77.9	0.1
M6	20	2	77.7	0.3
M7	20	2	77.5	0.5
M8	20	2	77.3	0.7

2.2 Characterization

2.2.1 Membrane performance

The pure water flux (PWF) of both pristine and TiO_2 NW/Fe_2O_3 functionalized PES membranes was evaluated using a custom-built crossflow filtration system [26]. The effective membrane filtration area was 13.69 cm^2. Before conducting filtration experiments, each membrane was compacted with DI water for at least 30 min under 4 bar until a stable flux was achieved. The pressure was reduced to 3 bar operating pressure, and the filtration tests were then performed. To ensure accuracy, the water permeability measurements were repeated three times, and the average values were reported. The PWF, expressed in $L/m^2 \cdot h$, was calculated using the following equation:

$$PWF = \Delta V / \left(\Delta t \times A \right), \quad (1)$$

where A refers to the effective membrane area (m^2), Δt refers to the permeation duration (h), and ΔV refers to the volume of permeate collected (L).

In the current study, NBB dye was selected as a model contaminant for evaluating the membrane performance. The filtration process was conducted at a constant pressure 1 bar and a temperature 25 ± 1 °C, using dye solutions with concentrations 25, 50, 100, and 150 mg/L and a pH range 3-12. Likewise, the impact of the nanoadditive amount on the manufactured membranes' performance was examined. Employing UV-Vis spectrophotometry (Shimadzu-UV160A, Japan), the dye concentration in the feed and permeate solutions was measured at a wavelenght of 620 nm. The following formula was used for estimating the membranes' dye rejection efficiency:

$$R\left(\%\right) = 1 - \left(\frac{C_p}{C_f} \right) \times 100, \quad (2)$$

where C_f is the solute concentration in the feed, C_p is the solute concentration in the permeate and R (%) is the membrane rejection rate.

Additionally, the flux recovery ratio (FRR) of the membranes was evaluated using 100 mg/L NBB dye solutions. The FRR, which indicates the membrane's potential to recover its original permeability after a filtration and cleaning cycle, was measured as follows:

$$FRR\left(\%\right) = \left(\frac{J_2}{J_1} \right) \times 100, \quad (3)$$

where J_1 and J_2 refer to the water flux before and after the filtration process, respectively.

2.2.2 Simulations

In this study, Design-Expert® software [27] was harnessed for experimental design and analysis. A historical data RSM design was implemented to connect and optimize three key operation parameters influencing the flux and rejection efficiency of the control and modified membranes. The historical data design approach permits flexible selection of experimental data points, making it particularly advantageous when working with pre-existing data [27–30]. Compared to any other RSM design type, historical data design has no constraints on the number of factors that could be employed, which facilitates unlimited analysis and optimization of membrane performance. For this study, the three independent variables examined were (A) concentration of TiO_2 NW/Fe_2O_3 (0.1 to 0.7 g), (B) NBB dye concentration (25-100 mg/L), and (C) pH level (3-12) (Table 2). The impact of these parameters on membrane flux and dye rejection efficiency was analyzed systematically using RSM. The optimal conditions were defined based on their statistical significance and interaction effects.

3 Results and discussion

3.1 Membrane filtration experiment results

Fig. 1 presents the PWF data for both the control PES membrane and the nanocomposite membranes incorporating different amounts of TiO_2 NWs-Fe_2O_3. A clear trend of increasing permeability is observed with higher nanostructure content. The neat PES membrane showcased the lowest PWF at 68 L/m^2·h. However, incorporating a small amount (0.01 g) of TiO_2 NWs-Fe_2O_3 into the polymer matrix resulted in a noticeable improvement, increasing the PWF to 60 L/m^2·h. This trend continued as the nanostructure content increased, with the M8 membrane, which contained 0.7 g of TiO_2 NWs-Fe_2O_3, demonstrating the highest PWF of 93 L/m^2·h. The significant enhancement in water flux can be attributed to the improved surface properties of the nanocomposite membranes, primarily increased hydrophilicity and porosity.

3.2 Optimizing of operating conditions

The permeate flux and retention performance following the incorporation of various concentrations of nanostructures in the membranes were evaluated under different feed solution concentrations and pH conditions. To determine the optimal operating conditions for nanocomposite membrane performance, NBB dye permeation and separation experiments were performed using feed concentrations of 25, 50, 100, and 150 mg/l at a pH range of 3 to 12.

As shown in Fig. 2(a), permeation flux declined by almost one-fifth when filtering a 25 mg/l NBB solution. This trend

Table 2 Experimental design data of TiO_2 NW/Fe_2O_3–PES nanocomposite membranes for dye removal

Run	Added TiO_2 NW/Fe_2O_3 (g)	Initial dye conentration (mg/L)	pH	Flux (L/m^2·h)	Rejection (%)
1	0.01	50.00	3.00	99.2	44
2	0.01	100.00	3.00	98.7	40
3	0.03	25.00	3.00	99.6	48
4	0.03	50.00	3.00	99.2	46
5	0.03	100.00	3.00	98	41
6	0.05	25.00	3.00	99.6	49
7	0.05	50.00	3.00	99.2	48
8	0.05	75.00	3.00	98.8	46
9	0.05	100.00	3.00	98.8	44
10	0.07	50.00	3.00	99.2	49
11	0.07	75.00	3.00	99.2	48
12	0.07	100.00	3.00	98.8	45
13	0.10	25.00	3.00	99.6	52
14	0.10	50.00	3.00	99.6	50
15	0.10	75.00	3.00	99.6	49
16	0.10	100.00	3.00	98.8	48
17	0.30	25.00	3.00	99.6	53
18	0.30	50.00	3.00	99.4	52
19	0.30	75.00	3.00	99.2	50
20	0.30	100.00	3.00	98.4	49
21	0.50	25.00	3.00	99.2	56
22	0.50	50.00	3.00	99.6	53
23	0.70	25.00	3.00	99.6	77
24	0.70	50.00	3.00	99.6	73
25	0.70	75.00	3.00	99.2	70
26	0.70	100.00	3.00	99.6	68
27	0.01	100.00	3.00	99.5	41
28	0.01	100.00	12.00	89	16
29	0.03	100.00	3.00	98	44
30	0.03	100.00	5.00	96	37
31	0.03	100.00	7.00	94	31
32	0.03	100.00	9.00	92	25
33	0.03	100.00	12.00	90	18
34	0.05	100.00	3.00	98.8	46
35	0.05	100.00	5.00	97	39
36	0.05	100.00	7.00	95	33
37	0.05	100.00	9.00	93	25
38	0.07	100.00	3.00	99.2	48
39	0.50	100.00	3.00	98.4	51
40	0.50	100.00	7.00	95	43
41	0.50	100.00	9.00	94	38
42	0.70	100.00	3.00	99.2	70
43	0.70	100.00	5.00	97	66
44	0.70	100.00	7.00	96	55
45	0.70	100.00	9.00	95	48
46	0.70	100.00	12.00	93	40

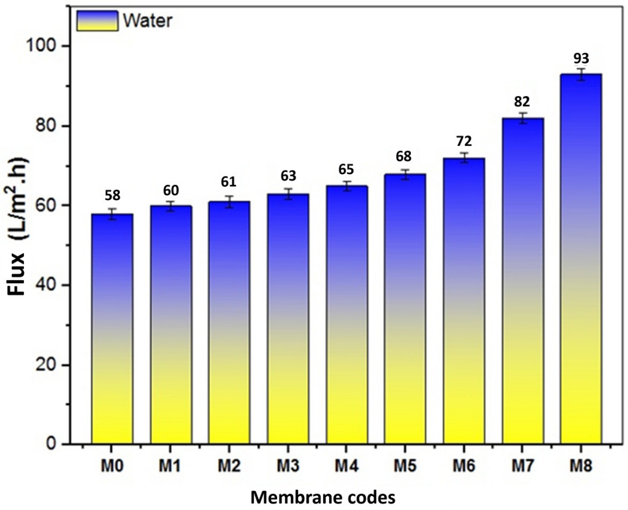

Fig. 1 The pure water flux (PWF) of membranes

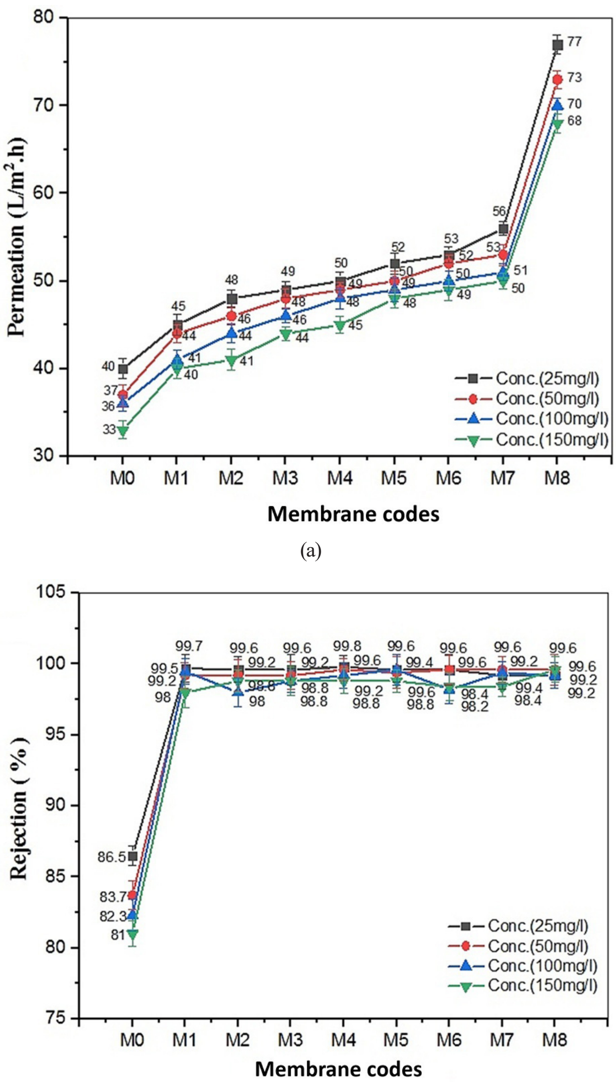

(a)

(b)

Fig. 2 Dye separation performance. (a) NBB permeation, (b) Dye separation performance

continued as the dye concentration increased, leading to a further decrease in flux, reaching about a one-third reduction when the feed solution was 150 mg/L. The reduction in permeability at higher dye concentrations can be ascribed to the membrane surface's compacted dye layer development, which introduced additional resistance to water passage and ultimately resulted in lower permeate flux.

Meanwhile, Fig. 2(b) illustrates the retention performance of the membranes against varying NBB dye concentrations. The unmodified PES membrane demonstrated the lowest rejection efficiency, ranging from 81% to 86.5%, whereas the TiO_2 NW/Fe_2O_3 nanocomposite membranes exhibited significantly enhanced removal rates, exceeding 98-99.7% for the M1 membrane and 99.2-99.6% for the M8 membrane, depending on the feed concentration. Notably, all modified membranes (M1 to M8) achieved similar and near-complete dye retention. This increase in separation efficiency can be attributed to rapid fouling, particularly even at low dye concentrations. Since NBB dye molecules are smaller than the membrane pores, they readily accumulated and caused pore blockage. This led to the development of a dense "cake layer" on the surface, which acted as an additional filtration barrier, preventing further dye penetration. Consequently, the presence of this layer played a crucial role in the high rejection efficiency observed in the nanocomposite membranes.

Likewise, the effect of pH solution on the permeation and removal characteristics of the nanocomposite membranes prepared with various amounts of nanostructure was illustrated in Fig. 3. The results demonstrate a clear impact of pH on the membrane's performance for NBB removal, with significant variations in both permeation and rejection rate. The permeation data (Fig. 3(a)) showcased that water flux declined with increasing the value of pH, where the highest permeation was witnessed at pH 3 and the lowest at pH 12. This could be induced by acidic conditions, which enhanced membrane hydrophilicity and diminished resistance to water flow. In contrast, under highly alkaline conditions (pH 12), membrane fouling and structural degradation can increase resistance, leading to a significant decline in permeation rate. These results align with previous studies [31, 32].

The rejection rate (Fig. 3(b)) follows an opposite trend, where dye removal efficiency is highest at lower pH levels (3-5) and decreases at pH 9-12. This can be ascribed to the dye molecules' electrostatic interactions with the membrane surface. As reported by literature [33, 34], NBB dye molecules are typically anionic, meaning it carries a negative charge in solution under most experimental

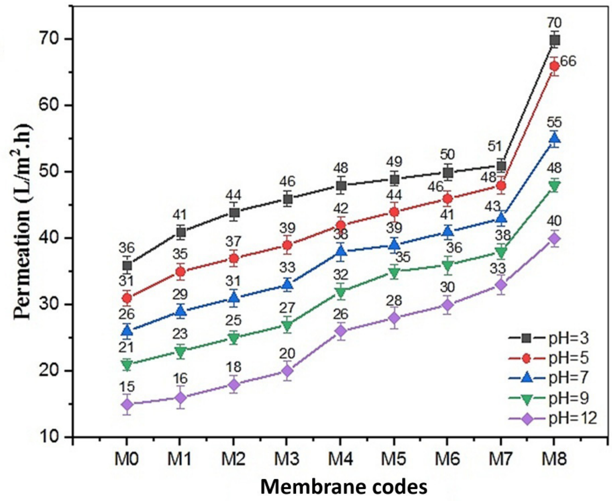

(a)

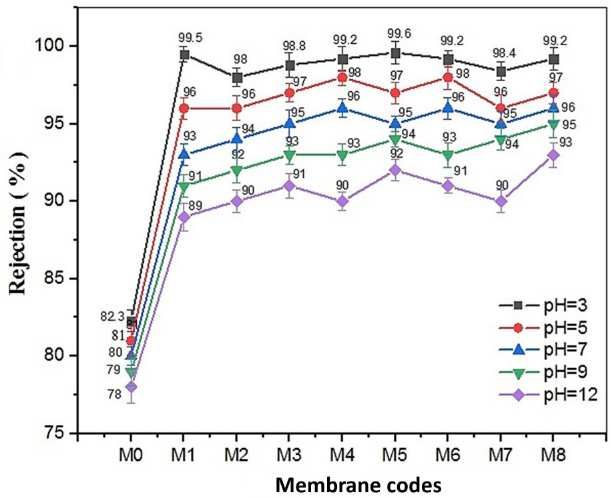

(b)

Fig. 3 Effect of NBB Dye solution pH on (a) permeation and (b) separation characteristics of the nanocomposite

pH conditions. Meanwhile, PES has slight negative charge under the entire pH range [6], which is also close to what reported for the nanocomposite in literature [35, 36]. Herein, under acidic pH conditions, membranes with a slight positive charge increased dye adsorption and rejection. In contrast, charge repulsion occurs between the membrane surface and the negatively charged dye molecules, inducing a decline in rejection efficiency at alkaline pH. Moreover, extreme pH conditions can alter the membrane's surface properties, influencing pore size and fouling characteristics, which might explain the observed performance drop at high pH [37]. These modifications likely enhance rejection rates while maintaining reasonable permeation, making them more reliable for dye wastewater treatment applications across different pH conditions. Overall, these findings reinforce the importance of optimizing membrane characteristics based on pH conditions to achieve the best balance between permeation and rejection efficiency.

3.3 Antifouling and long-term performance of nanocomposite membrane

The FRR, an important indication of irreversible fouling, was harnessed to assess the membranes' antifouling characteristics. The PWF of the membranes was calculated both prior to and following NBB dye filtering tests in order to determine the FRR. Membrane fouling frequently occurs as a result of solute accumulation during filtration. Effective antifouling behavior is demonstrated by higher FRR values in conjunction with relatively high NBB dye retention. The unmodified PES membrane displayed the lowest FRR, at 57%, as seen in Fig. 4(a). In contrast, the FRR of the membranes effectively enhanced the incorporation of TiO_2 NW/Fe_2O_3 nanostructures into the PES matrix. Particularly, the nanocomposite membrane prepared with 0.7 g nanostructure revealed an FRR of 73.4%, referring to significant enhancement in antifouling performance.

On the other hand, five cycles of prolonged filtration experiments were carried out for neat PES (M0) and M8 membranes with the objective to establish the best membrane's long-term performance, as shown in Fig. 4(b). The purpose of these tests was to evaluate the synthetic membranes' stability and lifespan over a 25 h operating duration. Every cycle involved measuring the permeation flux for 5 h, evaluating the reduction in permeation flux of an NBB dye solution, and then measuring the permeation flux of a backwashing step. After five cycles of filtration of the NBB dye solution, the permeation flow of both membranes revealed a gradual decline. After the fifth cycle of NBB dye filtration, the permeation flux of M0 and M8 diminished from 58 to 43 $L/m^2 \cdot h$ and from 93 to 77 $L/m^2 \cdot h$, respectively. The accumulation of NBB dye molecules on the surface of the membrane after extended filtration is thought to be the cause of this decrease [38]. When compared to the M8 modified membrane, the clean PES membrane showed a noticeable and almost irreversible drop in flow. The observed variations in the fouling trend demonstrate how crucial the membrane's surface features – such as porosity, pore size, and hydrophilicity – are to its antifouling characteristics.

The impact of the presence of TiO_2 NW/Fe_2O_3 in the polymeric matrix on the stability of the PES–TiO_2 NW/Fe_2O_3 membranes in the NBB dye removal system is illustrated in Fig. 4(c). It is apparent that the NBB dye adsorbs onto the membrane surface, inducing a progressive decrease in

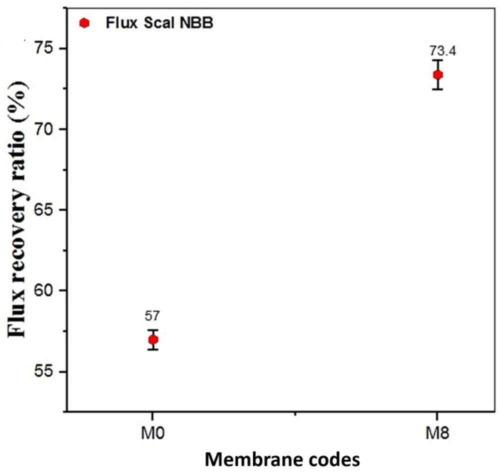

(a)

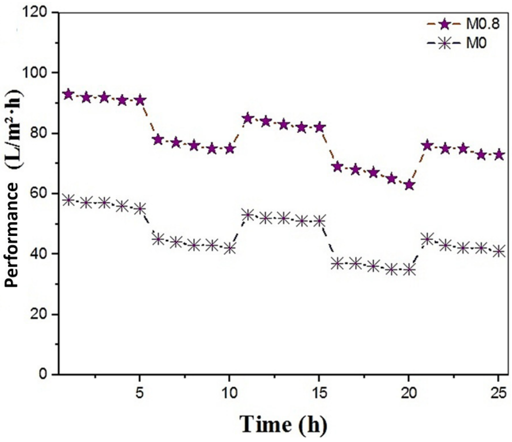

(b)

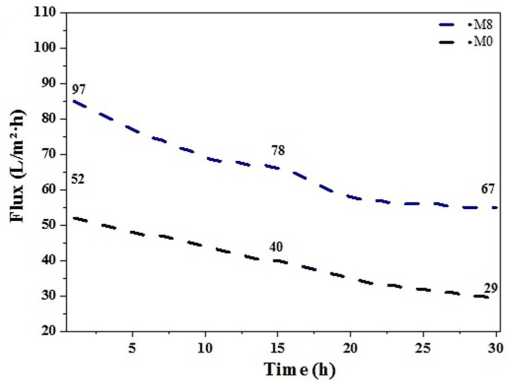

(c)

Fig. 4 (a) The flux recovery ratio (FRR) of M0 and M8 for 100 mg/L NBB dye solution; (b) Time-dependent flux of pure water and NBB dye solution for M0 and M8 membranes; (c) Stability operation for M0 and M8 membranes

the membrane's permeance performance over time when it is made from pristine PES. After 18 h of operation, the best membrane's permeability, which was fabricated from 0.7 g of TiO_2 NW/Fe_2O_3 in PES solution, started to stabilize. This observation shows that the inserted TiO_2 NWs-Fe_2O_3 made the fouling more reversible. This could support our theory that the membrane permeance becomes more stable when TiO_2 NW/Fe_2O_3 are embedded in PES solution. These results generally highlight the PES–TiO_2 NW/Fe_2O_3 membrane's potential for efficient dye separation and notable stability under operational conditions.

3.4 Statistical validation of the model (ANOVA analysis)

The analysis of variance (ANOVA) was utilized to validate the developed mathematical model and assess the statistical significance of the independent variables influencing flux and rejection efficiency. As presented in Tables 3 and 4, the ANOVA results indicate that the quadratic model is highly significant, with F-values of 298.76 for flux and 527.15 for rejection, both having p-values below 0.05, confirming statistical significance at a 95% confidence level. The determination coefficients (R^2 values) of 0.9668 and 0.9809 for flux and rejection, respectively, indicate that the model accounts for 96.68% and 98.41% of the variability in dye removal efficiency, leaving only a small fraction unexplained. Additionally, the "Pred R-squared" values (0.9582 and 0.9752) were in agreement with the "Adj R-squared" values (0.9636 and 0.9791), confirming the model's robustness. Furthermore, the "Adeq precision" values of 70.574 and 79.629, which exceed the desirable threshold of 4, confirm that the signal-to-noise ratio is sufficient for navigating the design space. Fig. 5 showcases the predicted versus actual values for permeate flux and retention. The close alignment between predicted and experimental values for both flux and rejection ($R^2 > 0.96$) validates the model's accuracy. However, minor deviations suggest that factors like membrane fouling or nanostructure aggregation (observed experimentally) may introduce slight variability.

The quadratic regression equations derived using Design-Expert® 13 software effectively describe the relationship between the process variables and responses. The model equations are as follows:

$$\text{Flux} = +37.57 + 11.99 \times A - 2.45 \times B - 14.02 \times C + 7.36 \times A^2 \tag{4}$$

$$\text{Rejection}(\%) = 95.32 + 0.92A - 0.43B - 3.90C + 0.83A \times C, \tag{5}$$

where A represents the TiO_2 NW/Fe_2O_3 concentration, B is the dye concentration, and C is the pH.

Table 3 ANOVA analysis of the flux

Source	Sum of squares	Degrees of freedom	Mean square	*F* value	*p*-value prob > *F*	Effect
Model	7199.01	4	1799.75	298.76	< 0.0001	
Additive concentration (g)	3835.12	1	3835.12	636.64	< 0.0001	
B-initial conentration	121.44	1	121.44	20.16	< 0.0001	
C-pH	2653.05	1	2653.05	440.41	< 0.0001	significant
Square additive concentration	226.98	1	226.98	37.68	< 0.0001	
Residual	246.99	41	6.02			
Lack of fit	233.49	36	6.49	2.40	0.1657	
Pure error	13.50	5	2.70			
Contour total	7446.00	45				
Standard deviation	2.45	R-squared	0.9668	Standard deviation	2.45	not significant
Mean	47.00	Adjusted R-squared	0.9636	Mean	47.00	
Coefficient of variation (CV) (%)	5.22	Predicted R-squared	0.9582	CV (%)	5.22	
Press coefficient	311.55	Adequate precision	70.574	Press coefficient	311.55	

Table 4 ANOVA analysis of the rejection %

Source	Sum of squares	Degrees of freedom	Mean square	*F* value	*p*-value prob > *F*	Effect
Model	333.39	4	83.35	527.15	< 0.0001	
Additive concentration (g)	13.74	1	13.74	86.89	< 0.0001	
B-initial con.	3.80	1	3.80	24.06	< 0.0001	
C-pH	191.23	1	191.23	1209.53	< 0.0001	significant
Additive concentration × pH value	8.26	1	8.26	52.24	< 0.0001	
Dye concentration × pH value	0.000	0				
Residual	6.48	41	0.16			
Lack of fit	6.00	36	0.17	1.74	0.2819	
Pure error	0.48	5	0.096			
Contour total	339.87	45				
Standard deviation	0.40	R-squared	0.9809			not significant
Mean	97.57	Adjusted R-squared	0.9791			
CV (%)	0.41	Predicted R-squared	0.9752			
Press coefficient	8.42	Adequate precision	79.629			

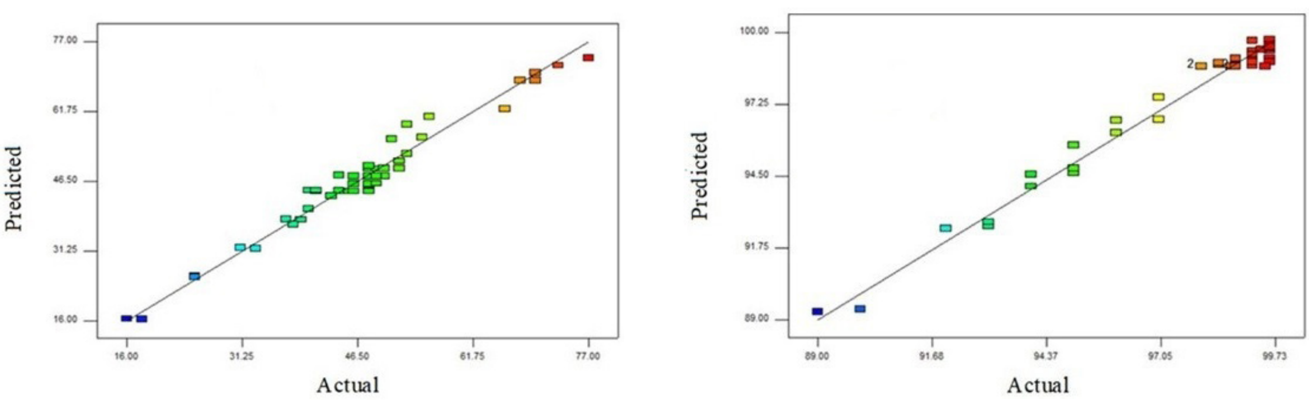

(a) (b)

Fig. 5 Predicted and actual results for the (a) flux and (b) rejection %

3.4.1 Effect of independent variables on flux and rejection

Fig. 6 demonstrates how the effects of the experimental variables and their interactions were examined using Design-Expert® software. The One Factor Plot analysis demonstrates that when one factor varies while others remain constant, the slope of the curve determines the strength of its effect. A slope of one indicates a more pronounced influence on the membrane performance, while a zero slope suggests minimal impact [39, 40].

Figs. 6(a) and 6(b) show the effect of TiO_2 NW/Fe_2O_3 concentration on flux and rejection at a fixed pH of 7.5 and dye concentration of 62.5 mg/L. Increasing the additive concentration from 0 to 0.7 wt.% resulted in a

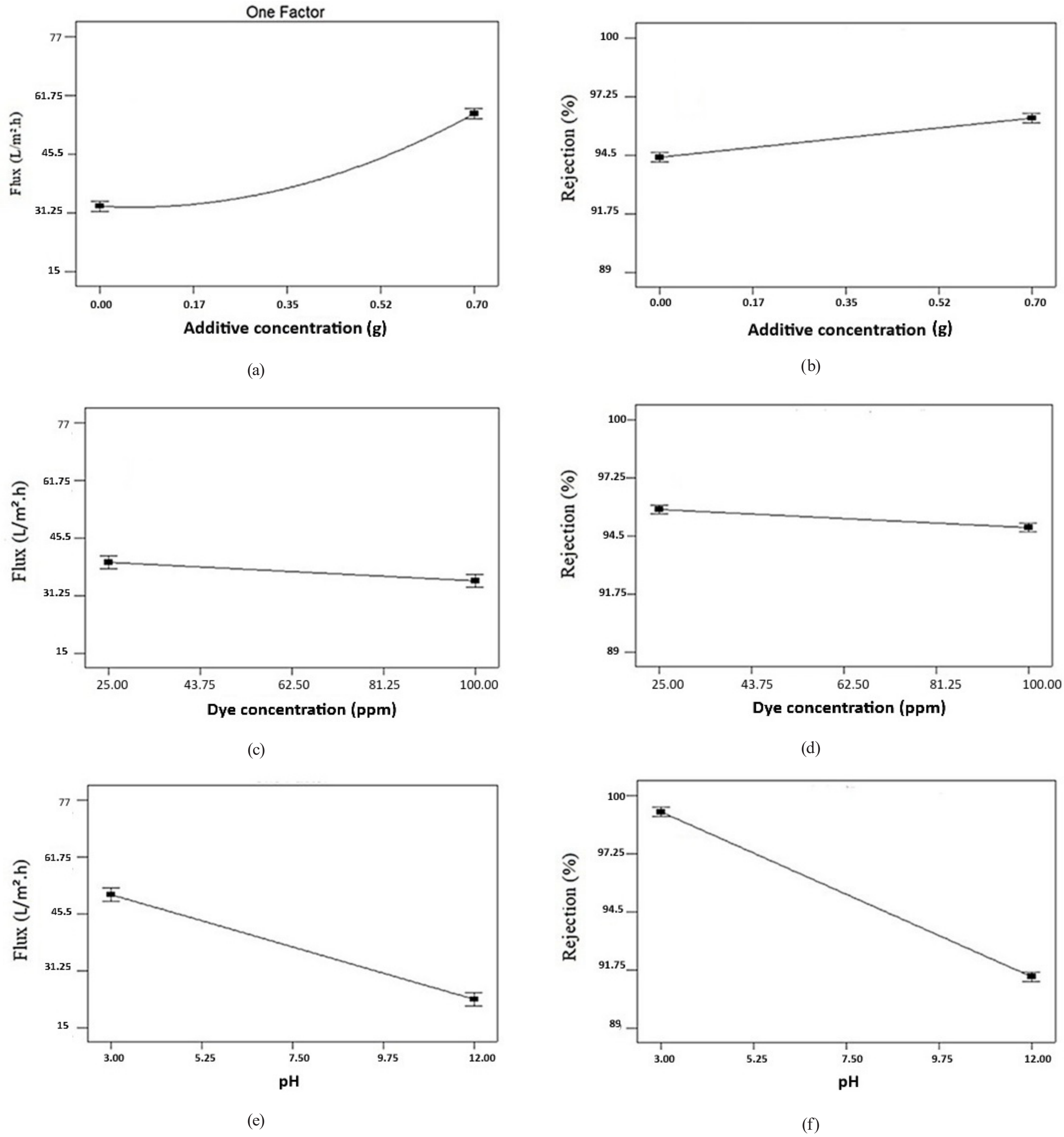

Fig. 6 Influence of variables on the membrane performance: (a) effect of additive concentration (g) on membrane flux; (b) effect of additive concentration (g) on membrane rejection; (c) effect of dye concentration (ppm) on membrane flux; (d) effect of dye concentration (ppm) on membrane rejection; (e) effect of pH value on membrane flux; (f) effect of pH value on membrane rejection

significant increase in flux and rejection. This enhancement is attributed to improved membrane porosity, larger average pore size, and increased hydrophilicity, which facilitate higher water permeability and effective dye rejection. These findings align with previous research that demonstrated how incorporating nanomaterials into polymeric membranes enhances permeability and selectivity through surface modifications and structural changes.

Figs. 6(c) and 6(d) illustrate the effect of dye concentration on flux and rejection % for membranes at a fixed pH 7.5 and an additive concentration 0.35 g. As the dye concentration increased from 25 to 100 mg/L, both flux and rejection efficiency declined. This reduction in flux can be explained by the dye molecules that have accumulated on the membrane surface, forming a thin, compact layer that hinders water permeability.

Meanwhile, the solution pH had a strong influence on both flux and rejection efficiency, as shown in Figs. 6(e) and 6(f). As pH increased from 3 to 12, the flux declined from 51.6 to 23.5 $L/m^2 \cdot h$, while separation decreased from 78.55% to 38.9%. The significant decline in rejection efficiency can be determined by the way the NBB dye interacts with the chemistry of the membrane surface at various pH values. At acidic conditions (pH = 3), the PES polymer chains interact strongly with the NBB dye via hydrogen bonding, electrostatic interactions, and π-π stacking. The sulfonyle $(-S(=O)_2^-)$ and ether (−O−) groups present in PES act as hydrogen bond acceptors, while the hydroxyl (−OH) and sulfonic acid ($-SO_3H$) groups in NBB serve as hydrogen bond donors. Additionally, the negative sulfonate $(-S_3^-)$ groups in NBB interact electrostatically with positively charged sites on the PES membrane, enhancing rejection efficiency. Conversely, at alkaline conditions (pH = 12), PES remains neutral and hydrophobic, while NBB is an anionic dye. The electrostatic interactions weaken significantly, leading to reduced dye retention and increased permeability.

3.4.2 Variables combined influence on the flux and rejection %

The interaction of key operational variables – additive concentration, NBB dye concentration, and pH – was systematically evaluated to optimize membrane performance in terms of flux and separation percentage. The RSM analysis provided critical insights into the complex relationships between these variables and their impact on membrane efficiency.

The combined influence of additive and dye concentration revealed that flux consistently increased with higher TiO_2 NW/Fe_2O_3 loading (0.01 to 0.7 g) across all dye concentrations (Figs. 7(a) and 7(b)). This improvement can be assigned to the enhancement in hydrophilicity and porosity resulting from the nanostructures, which facilitated greater water permeability. While flux showed a slight decline at the highest dye concentration (100 mg/L) due to fouling, the presence of additives helped mitigate this effect by reducing dye adhesion to the membrane surface. In terms of rejection, the membranes maintained excellent performance, exceeding 95% rejection across all conditions. The nanostructures' ability to attract anionic NBB dye molecules, combined with pore-size exclusion, contributed to this consistently high rejection rate, with only marginal improvements observed at the highest additive loads.

The interaction between additive concentration and pH demonstrated that while increasing additive loading positively affected performance at all pH levels, the benefits were most pronounced under acidic conditions (pH 3-5) (Figs. 7(c) and 7(d)). At pH 3, both flux and rejection reached their peak values. This was likely due to the protonation of membrane surface groups, which enhanced dye adsorption, and the reduction of electrostatic repulsion between the anionic NBB dye and the membrane surface. In contrast, performance deteriorated significantly under highly alkaline conditions (pH 12), where rejection dropped to less than 25% at the lowest additive concentration.

When examining the effects of pH and dye concentration at a fixed additive loading (0.35 g), the parallel contours in the response surface plots indicated that these two variables acted independently (Figs. 7(e) and 7(f)). This finding suggests that at intermediate additive concentrations, pH is the dominant factor affecting membrane performance, while dye concentration primarily influences the extent of fouling. The consistent drop in performance at alkaline pH, even at low dye concentrations, further underscores the critical role of pH in determining membrane–dye interactions.

3.5 Optimization and model validation

The optimal conditions relied on a desirability value of one. The optimization process identified 0.7 g additive loading, 51.54 mg/L dye concentration, and pH 3 as the ideal conditions, predicting a flux of 71.65 $L/m^2 \cdot h$ and 99.43% rejection (Fig. 8). Experimental validation of these conditions yielded 72.55 $L/m^2 \cdot h$ and 99% rejection, demonstrating the model's accuracy (error < 2%). However, despite SEM observations of nanoparticle aggregation at the 0.7 g additive, it might still offer

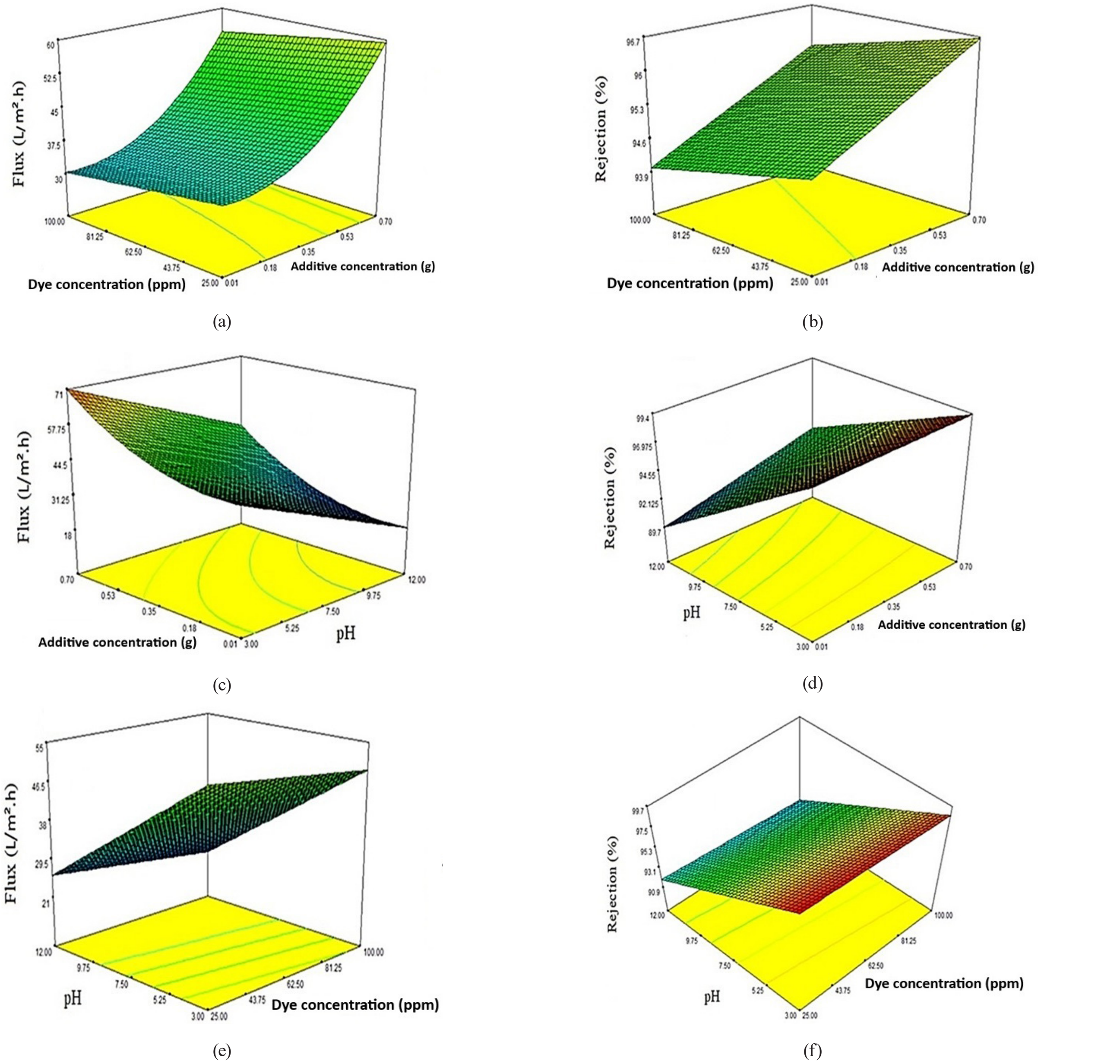

Fig. 7 Influence of variables on the membrane performance: (a) constant pH (flux); (b) constant pH (rejection); (c) constant dye concentration (ppm) (flux); (d) constant dye concentration (ppm) (rejection); (e) constant additive concentration (flux); (f) constant additive concentration (rejection)

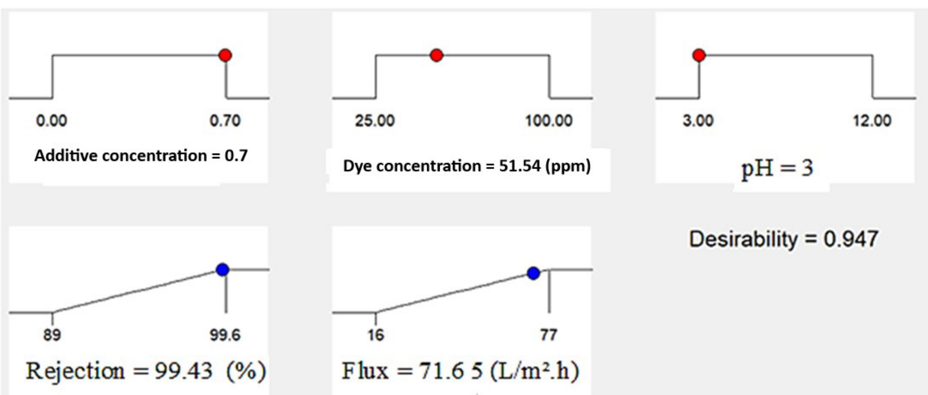

Fig. 8 Desirability ramp for the numerical optimization of three chosen factors

a better balance between performance and membrane integrity in practical applications. While pH 3 provided optimal results, a slightly higher range (pH 3-5) may be more feasible for industrial implementation.

The RSM analysis has provided valuable insights into the complex interplay of factors affecting membrane performance. The model's accuracy, as demonstrated by the close agreement between predicted and experimental results, supports its use for scaling up membrane processes. The findings highlight the importance of carefully balancing additive concentration and pH to achieve optimal performance while maintaining membrane stability. For industrial applications, a moderate additive load (0.7 g) and slightly acidic conditions (pH 3-5) may represent the most practical compromise between performance and operational feasibility. These results provide a solid foundation for the development of efficient membrane-based systems for dye removal from industrial wastewater.

4 Conclusion

The RSM model confirmed that additive concentration and pH play critical roles in membrane performance. The optimized membrane composition (0.7 g TiO_2 NW/Fe_2O_3) manifested high permeability (93 L/m^2·h) and dye removal efficiency of more than 99%, making it a promising candidate for dye separation applications. Meanwhile, acidic conditions (pH 3-5) promoted strong electrostatic interactions between the membrane and dye molecules, enhancing rejection, while alkaline pH reduced performance due to charge repulsion effects. Under optimized conditions (0.7 g additive, pH 3, 51.54 mg/L dye), the membrane maintained >99% retention, aligning with experimental results (M8 membrane). Besides that, simulation analyses provided deeper insights into the dye removal mechanisms across varying pH conditions, supporting the experimental findings. Obtained results shed light on the importance of balancing nanostructure incorporation and pH control to optimize membrane performance. The TiO_2 NW/Fe_2O_3-modified PES membranes present a promising solution for efficient dye removal in industrial wastewater treatment, contributing to the advancement of sustainable and high-performance membrane technologies.

Acknowledgments

Prof. Dr. Qusay F. Alsalhy gratefully thanks Dr. Mohammed Ahmed Shehab, Dr. Zoltan Nemeth, and Prof. Klara Hernadi, University of Miskolc, H-3515 Miskolc, Hungary, for their assistance in preparing the TiO_2 NW/Fe_2O_3.

References

[1] Akbari, A., Remigy, J. C., Aptel, P. "Treatment of textile dye effluent using a polyamide-based nanofiltration membrane", Chemical Engineering and Processing: Process Intensification, 41(7), pp. 601–609, 2002. https://doi.org/10.1016/S0255-2701(01)00181-7

[2] Keskin, B., Ersahin, M. E., Ozgun, H., Koyuncu, I. "Pilot and full-scale applications of membrane processes for textile wastewater treatment: A critical review", Journal of Water Process Engineering, 42, 102172, 2021. https://doi.org/10.1016/j.jwpe.2021.102172

[3] Ahmad, A. L., Harris, W., Syafiie, S., Seng, O. "Removal of Dye From Wastewater of Textile Industry Using Membrane Technology", Jurnal Teknologi, 36, pp. 31–44, 2002.

[4] Al-Araji, D. D., Al-Ani, F. H., Alsalhy, Q. F. "Modification of polyethersulfone membranes by Polyethyleneimine (PEI) grafted Silica nanoparticles and their application for textile wastewater treatment", Environmental Technology, 44(20), pp. 3033–3049, 2023. https://doi.org/10.1080/09593330.2022.2049890

[5] Moradihamedani, P. "Recent advances in dye removal from wastewater by membrane technology: a review", Polymer Bulletin, 79(4), pp. 2603–2631, 2022. https://doi.org/10.1007/s00289-021-03603-2

[6] Al Aani, S., Wright, C. J., Hilal, N. "Investigation of UF membranes fouling and potentials as pre-treatment step in desalination and surface water applications", Desalination, 432, pp. 115–127, 2018. https://doi.org/10.1016/j.desal.2018.01.017

[7] Al Aani, A., Wright, C. J., Atieh, M. A., Hilal, N. "Engineering nanocomposite membranes: Addressing current challenges and future opportunities", Desalination, 401, pp. 1–15, 2017. https://doi.org/10.1016/j.desal.2016.08.001

[8] Abood, T., Shabeeb, K., Alzubaydi, A., Goh, P., Ismail, A., Zrelli, A., Alsalhy, Q. "Effect of MXene Ti_3C_2 on the PVDF ultrafiltration membrane properties and performance", Engineering and Technology Journal, 42(6), pp. 754–767, 2024. http://doi.org/10.30684/etj.2024.145778.1663

[9] Al Aani, S., Gomez, V., Wright, C. J., Hilal, N. "Fabrication of antibacterial mixed matrix nanocomposite membranes using hybrid nanostructure of silver coated multi-walled carbon nanotubes", Chemical Engineering Journal, 326, pp. 721–736, 2017. https://doi.org/10.1016/j.cej.2017.06.029

[10] Al-Araji, D. D., Al-Ani, F. H., Alsalhy, Q. F. "Polyethyleneimine (PEI) grafted silica nanoparticles for polyethersulfone membranes modification and their outlooks for wastewater treatment-a review", International Journal of Environmental Analytical Chemistry, 103(16), pp. 4752–4776, 2023. https://doi.org/10.1080/03067319.2021.1931163

[11] Al Aani, S., Haroutounian, A., Wright, C. J., Hilal, N. "Thin Film Nanocomposite (TFN) membranes modified with polydopamine coated metals/carbon-nanostructures for desalination applications", Desalination, 427, pp. 60–74, 2018. https://doi.org/10.1016/j.desal.2017.10.011

[12] Kadhim, R. J., Al-Ani, F. H., Alsalhy, Q. F. "MCM-41 mesoporous modified polyethersulfone nanofiltration membranes and their prospects for dyes removal", International Journal of Environmental Analytical Chemistry, 103(4), pp. 828–848, 2023. https://doi.org/10.1080/03067319.2020.1865326

[13] Al-Timimi, D. A. H., Alsalhy, Q. F., AbdulRazak, A. A. "Polyethersulfone/amine grafted silica nanoparticles mixed matrix membrane: A comparative study for mebeverine hydrochloride wastewater treatment", Alexandria Engineering Journal, 66, pp. 167–190, 2023. https://doi.org/10.1016/j.aej.2022.11.044

[14] Ali, A. M., Rashid, K. T., Yahya, A. A., Majdi, H. S., Salih, I. K., Yusoh, K., Q.F. Alsalhy, Q. F., AbdulRazak, A. A., Figoli, A. "Fabrication of gum arabic-graphene (GGA) modified polyphenylsulfone (PPSU) mixed matrix membranes: A systematic evaluation study for ultrafiltration (UF) applications", Membranes, 11(7), 542, 2021. https://doi.org/10.3390/membranes11070542

[15] Kumar, M. A., Abebe, B., Nagaswarupa, H., Murthy, H. A., Ravikumar, C., Sabir, F. K. "Enhanced photocatalytic and electrochemical performance of TiO_2-Fe_2O_3 nanocomposite: Its applications in dye decolorization and as supercapacitors", Scientific Reports, 10(1), 1249, 2020. https://doi.org/10.1038/s41598-020-58110-7

[16] Radwan, A., Mohamed, S. O., Khalil, M. M., El-Sewify, I. M. "Effective adsorption of fluorescent congo red azo dye from aqueous solution by green synthesized nanosphere ZnO/CuO composite using propolis as bee byproduct extract", Scientific Reports, 14(1), 9061, 2024. https://doi.org/10.1038/s41598-024-58306-1

[17] Waqas, S., Bilad, M. R., Man, Z. B., Suleman, H., Nordin, N. A. H., Jaafar, J., Othman, M. H. D., Elma, M. "An energy-efficient membrane rotating biological contactor for wastewater treatment", Journal of Cleaner Production, 282, 124544, 2021. https://doi.org/10.1016/j.jclepro.2020.124544

[18] Deng, L., Guo, W., Ngo, H. H., Du, B., Wei, Q., Tran, N. H., Nguyen, N. C., Chen, S.-S., Li, J. "Effects of hydraulic retention time and bioflocculant addition on membrane fouling in a sponge-submerged membrane bioreactor", Bioresource Technology, 210, pp. 11–17, 2016. https://doi.org/10.1016/j.biortech.2016.01.056

[19] Ghadhban, M. Y., Rashid, K. T., Abdulrazak, A. A., Meskher, H., Benguerba, Y., Al-Sarraj, E. A. Y., Alsalhya, Q. F. "Optimal operational conditions of PLA/PBAT mixed matrix membrane for the treatment of oily wastewater", Engineering and Technology Journal, 42(9), pp. 1179–1192, 2024. http://doi.org/10.30684/etj.2024.150993.1774

[20] Al-Timimi, D. A. H., Alsalhy, Q. F., AbdulRazak, A. A., Shehab, M. A., Németh, Z., Hernadi, K. "Optimum operating parameters for PES nanocomposite membranes for mebeverine hydrochloride removal", Journal of Materials Research and Technology, 24, pp. 6779–6790, 2023. https://doi.org/10.1016/j.jmrt.2023.04.247

[21] Abdulgader, M., Yu, Q. J., Zinatizadeh, A. A., Williams, P., Rahimi, Z. "Application of response surface methodology (RSM) for process analysis and optimization of milk processing wastewater treatment using multistage flexible fiber biofilm reactor", Journal of Environmental Chemical Engineering 8(3), 103797, 2020. https://doi.org/10.1016/j.jece.2020.103797

[22] Rajewski, J., Dobrzyńska-Inger, A. "Application of Response Surface Methodology (RSM) for the Optimization of Chromium(III) Synergistic Extraction by Supported Liquid Membrane", Membranes, 11(11), 854, 2021. https://doi.org/10.3390/membranes11110854

[23] Inger, M., Dobrzyńska-Inger, A., Rajewski, J., Wilk, M. "The use of response surface methodology in ammonia oxidation reaction study", Journal of Chemistry, 2019(1), 2641315, 2019. https://doi.org/10.1155/2019/2641315

[24] Shehab, M. A., Szőri-Dorogházi, E., Szabó, S., Valsesia, A., Chauhan, T., Koós, T., Muránszky, G., Szabó, T., Hernadi, K., Németh, Z. "Virus and bacterial removal ability of TiO_2 nanowire-based self-supported hybrid membranes", Arabian Journal of Chemistry, 16(1), 104388, 2023. https://doi.org/10.1016/j.arabjc.2022.104388

[25] Hussein, M. M., Alsalhy, Q. F., Alalm, M. G., El-Halwany, M. M. “Optimization of Developed TiO_2 NWs-Fe_2O_3 Modified PES Membranes for Efficient NBB Dye Removal”, ChemEngineering, 9(4), 82, 2025. https://doi.org/10.3390/chemengineering9040082

[26] Huang, J. H., Cheng, X. Q., Wu, Y. D., Zhang, Y. Q., Li, S. W., Lau, C. H., Shao, L. "Critical operation factors and proposed testing protocol of nanofiltration membranes for developing advanced membrane materials", Advanced Composites and Hybrid Materials, 4(4), pp. 1092–1101, 2021. https://doi.org/10.1007/s42114-021-00334-w

[27] IQC Quality Services "Design-Expert® V13", [computer program] Available at: https://www.iqcqs.org/?page_id=86 [Accessed: 04 May 2025]

[28] Daham, G. R., AbdulRazak, A. A., Hamadi, A. S., Mohammed, A. A. "Re-refining of used lubricant oil by solvent extraction using central composite design method", Korean Journal of Chemical Engineering, 34(9), pp. 2435–2444, 2017. https://doi.org/10.1007/s11814-017-0139-5

[29] Ahmed, F. S., AbdulRazak, A. A., Alsaffar, M. A. "Modelling and optimization of methylene blue adsorption from wastewater utilizing magnetic marble dust adsorbent: A response surface methodology approach", Materials Today: Proceedings, 60, pp. 1676–1688, 2022. https://doi.org/10.1016/j.matpr.2021.12.224

[30] Ali, N. N., Alayan, H. M., AbdulRazak, A. A., Jalil, R. R. "Modeling and optimizing phenol degradation in aqueous solution using post discharge DBD plasma treatment", Desalination and Water Treatment, 321, 100993, 2025. https://doi.org/10.1016/j.dwt.2025.100993

[31] Al-Dahri, T., Abdulrazak, A., Khalaf, I., Rohani, S. "Response surface modeling of the removal of methyl orange dye from its aqueous solution using two types of zeolite synthesized from coal fly ash", Materials Express, 8(3), pp. 234–244, 2018. https://doi.org/10.1166/mex.2018.1433

[32] Capar, G., Yilmaz, L., Yetis, U. "Reclamation of acid dye bath wastewater: Effect of pH on nanofiltration performance", Journal of Membrane Science, 281(1), pp. 560–569, 2006. https://doi.org/10.1016/j.memsci.2006.04.025

[33] Barredo-Damas, S., Alcaina-Miranda, M. I., Iborra-Clar, M. I., Mendoza-Roca, J. A., Gemma, M. "Effect of pH and MWCO on textile effluents ultrafiltration by tubular ceramic membranes", Desalination and Water Treatment, 27(1), pp. 81–89, 2011. https://doi.org/10.5004/dwt.2011.2057

[34] Alkhabbas, M., Al-Ma'abreh, A. M., Edris, G., Saleh, T., Alhmood, H. "Adsorption of anionic and cationic dyes on activated carbon prepared from oak cupules: Kinetics and thermodynamics studies", International Journal of Environmental Research and Public Health, 20(4), 3280, 2023. https://doi.org/10.3390/ijerph20043280

[35] Mahdi, N., Kumar, P., Goswami, A., Perdicakis, B., Shankar, K., Sadrzadeh, M. "Robust Polymer Nanocomposite Membranes Incorporating Discrete TiO_2 Nanotubes for Water Treatment", Nanomaterials, 9(9), 1186, 2019. https://doi.org/10.3390/nano9091186

[36] Paramo, L., Jiménez-Chávez, A., Medina-Ramirez, I. E., Böhnel, H. N., Escobar-Alarcón, L., Esquivel, K. "Biocompatibility Evaluation of TiO_2, Fe_3O_4, and TiO_2/Fe_3O_4 Nanomaterials: Insights into Potential Toxic Effects in Erythrocytes and HepG2 Cells", Nanomaterials, 13(21), 2824, 2023. https://doi.org/10.3390/nano13212824

[37] Guo, Q., Wu, X., Ji, Y., Hao, Y., Liao, S., Cui, Z., Li, J., Younas, M., He, B. "pH-responsive nanofiltration membrane containing chitosan for dye separation", Journal of Membrane Science, 635, 119445, 2021. https://doi.org/10.1016/j.memsci.2021.119445

[38] Tarun, S., Dakshesh, S., Arthanareeswaran, G. "Tuning of polymeric membranes to mitigate fouling and removal of dissolved compounds for wastewater treatment: A Review", Frontiers in Membrane Science and Technology, 3, 1389239, 2024. http://dx.doi.org/10.3389/frmst.2024.1389239

[39] Zhang, Y., Wang, Y., Wang, X., Zhang, Z., Li, S., Hu, Y., Gong, G. "Construction of robust one-dimensional nanowire-regulated graphene oxide membranes for efficient dye/salt separation", Journal of Membrane Science, 686, 122027, 2023. https://doi.org/10.1016/j.memsci.2023.122027

[40] Shakor, Z. M., AbdulRazak, A. A., Shuhaib, A. A. "Optimization of process variables for hydrogenation of cinnamaldehyde to cinnamyl alcohol over a Pt/SiO_2 catalyst using response surface methodology", Chemical Engineering Communications, 209(6), pp. 827–843, 2022. https://doi.org/10.1080/00986445.2021.1922394